PNAS RESEARCH ARTICLE | PSYCHOLOGICAL AND COGNITIVE SCIENCES NEUROSCIENCE

Visual adaptation stronger at the horizontal than the vertical meridian: Linking performance with V1 cortical surface area

Hsing-Hao Lee[a,1] and Marisa Carrasco[a,b,1]

Contributed by Marisa Carrasco; received April 2, 2025; accepted June 10, 2025; reviewed by Geoffrey Boynton and Michael A. Webster

Visual adaptation reduces bioenergetic expenditure by decreasing sensitivity to repetitive and similar stimuli. In human adults, visual performance varies systematically around the polar angle for many visual dimensions and tasks: Performance is superior along the horizontal than the vertical meridian (horizontal–vertical anisotropy, HVA) and the lower than upper vertical meridian (vertical meridian asymmetry, VMA). These asymmetries are resistant to spatial and temporal attention. However, it remains unknown whether visual adaptation differs around the polar angle. Here, we investigated how adaptation influences contrast sensitivity at the fovea and perifovea across the four cardinal meridian locations for both horizontal and vertical stimuli in an orientation discrimination task. In the nonadapted conditions, the HVA was more pronounced for horizontal than vertical stimuli. For both orientations, adaptation was stronger along the horizontal than the vertical meridian, exceeding foveal adaptation. Additionally, perifoveal adaptation effects positively correlated with individual V1 cortical surface area. These findings reveal that visual adaptation mitigates the HVA in contrast sensitivity, fostering perceptual uniformity around the visual field while conserving bioenergetic resources.

visual adaptation | contrast sensitivity | visual cortex | polar angle asymmetries

Visual performance exhibits systematic spatial variations across the visual field: Sensitivity declines with eccentricity (1–3) and varies systematically around the polar angle: Performance is superior along the horizontal than the vertical meridian (horizontal – vertical anisotropy, HVA) and along the lower than the upper vertical meridian (vertical meridian asymmetry, VMA). These asymmetries persist across multiple dimensions—e.g., contrast sensitivity (4–10), spatial resolution (11–15), motion (16–20), visual acuity (21, 22), perceived contrast (9), and perceived spatial frequency (23)—and mid-level and higher-order tasks, e.g., crowding (15, 24–27), texture segmentation (14, 15, 21, 22, 28), perceived object size (29), face perception (30, 31), short-term memory (23), and word identification (32). However, contrast sensitivity is the currency of the visual system, which most—if not all—visual dimensions depend upon to some degree.

Visual adaptation decreases sensitivity for stimuli that have been encountered repeatedly in the past, thereby increasing sensitivity to changes in the environment (33). Adaptation helps conserve the brain's limited bioenergetic resources by allocating less energy to repetitive stimuli (33–36). For instance, contrast adaptation reduces sensitivity (35–43) and neural responses (44–53), and shifts the contrast response function in V1 to recenter sensitivity away from the adaptor (54).

However, there is a spatial bias in adaptation studies: 1) Most studies have focused on horizontal meridian locations (e.g., 55, 56–58). 2) The few studies that tested other locations (e.g., intercardinal locations or vertical meridian) have not analyzed them separately (e.g., 43, 59). Thus, whether and how the adaptation effect varies around the polar angle remain unknown. 3) Moreover, the magnitude of the adaptation effect across eccentricity has yielded inconsistent findings; some show similar extent of adaptation with cortically magnified stimuli (40, 56), whereas others show parafoveal dominance (58, 59). Addressing these gaps will reveal how adaptation alters perception and conserves bioenergetic resources throughout the visual field.

Cortical magnification—the amount of cortical surface area corresponding to one degree of visual angle ($mm^2/°$)—declines with eccentricity (60–64) and has been used to link perceptual performance to brain structure. Converging neural evidence demonstrates that cortical magnification limits peripheral vision: V1 surface area across eccentricity correlates with various perceptual measures, including perceived object size (65, 66), perceived angular size (67), and acuity (68, 69). Moreover, V1 surface area around the polar angle also correlates with perceptual measures, including contrast sensitivity and acuity (70–72).

Significance

Human visual perception varies around the visual field, with robust horizontal–vertical and vertical meridian asymmetries. These asymmetries are pervasive—present for monocular and binocular viewing, different stimulus sizes, orientations, eccentricities, luminance levels—and resilient—they remain under conditions that improve perception, such as covert attention, and are even exacerbated with presaccadic attention. Here, we investigated whether visual adaptation, which helps manage bioenergetic resources, alters these polar angle asymmetries. We found that adaptation decreases the horizontal–vertical asymmetry, making perception more uniform across the visual field. Moreover, the degree of this effect correlates with the surface area in the primary visual cortex. This study reveals that a fundamental visual process—adaptation—diminishes this prominent perceptual asymmetry.

Author affiliations: [a]Department of Psychology, New York University, New York, NY 10003; and [b]Center for Neural Science, New York University, New York, NY 10003

Author contributions: H.-H.L. and M.C. designed research; H.-H.L. performed research; H.-H.L. analyzed data; M.C. supervised and obtained funding; and H.-H.L. and M.C. wrote the paper.

Reviewers: G.B., University of Washington; and M.A.W., University of Nevada Reno College of Science.

The authors declare no competing interest.

[1]To whom correspondence may be addressed. Email: hsinghaolee@nyu.edu. or marisa.carrasco@nyu.edu.

This article contains supporting information online at https://www.pnas.org/lookup/suppl/doi:10.1073/pnas.2507810122/-/DCSupplemental.

Published July 14, 2025.

Here, we investigated whether adaptation decreases contrast sensitivity similarly around the polar angle and at fovea using an orientation discrimination task. This task has been a proxy for contrast sensitivity because on this task performance monotonically increases with contrast (73). This task has been used this way in many studies (e.g., 6, 7, 10, 74–84), including adaptation studies (35, 42, 85). Here, we tested three hypotheses:

(1) Uniform adaptation: Similar adaptation magnitude across meridians, consistent with the central role of the early visual cortex in both adaptation (36, 42) and covert spatial attention (36, 84), and with the findings that attention improves performance similarly around the polar angle (86–89).
(2) Vertical meridian dominance: Stronger adaptation along the vertical (particularly the upper vertical meridian) than the horizontal meridian, as predicted by adaptor-target similarity (58, 59, 90) being stronger where population receptive fields (pRF) size is larger (72, 91, 92) and stimuli are less precisely encoded (93).
(3) Horizontal meridian dominance: Stronger adaptation along the horizontal than the vertical meridian (particularly upper), consistent with the larger cortical surface area devoted to the horizontal than the vertical meridian (63, 70–72, 91, 92). V1 neuronal density is approximately uniform across visual space (94, 95) and locations with more neurons devoted to sensory processing elicit a stronger response to the adaptor (96, 97), which amplifies the adaptation effect (54, 98–101). This prediction is consistent with the fact that adaptation increases with the strength of the response to the stimulus (102–105).

Fourteen adults participated in all three experiments (Fig. 1). Participants performed an orientation discrimination task, as in previous studies of contrast adaptation (35, 85, 104). In Experiment 1, participants adapted to a horizontal stimulus and discriminated whether a target Gabor—presented at the same location as the adaptor among one of four perifoveal cardinal locations—was tilted clockwise or counterclockwise from horizontal (Fig. 1*A*). Given that sensitivity to gratings is higher for radial than tangential orientations (106–108), we hypothesized an exacerbated HVA when the task involved horizontal stimulus orientation, which is radial at the horizontal meridian. To evaluate the influence of a radial bias, in Experiment 2 participants adapted to a vertical stimulus and discriminated whether a Gabor was tilted clockwise or counterclockwise from vertical. These experiments enabled us to 1) evaluate the role of cortical surface area in adaptation and 2) compare the extent of both HVA and VMA with different stimulus orientations.

In Experiment 3, we examined adaptation effects at the fovea using the same orientation discrimination tasks (Fig. 1*B*). This experiment enabled us to 1) further evaluate the role of cortical surface area in adaptation and 2) address previous inconsistent findings regarding task eccentricity-dependent adaptation effects (40, 56–59, 109–111): For instance, whereas tilt aftereffects are stronger for suprathreshold targets at peripheral than central vision along the horizontal meridian (57, 58, 109–111), contrast threshold adaptation shows comparable magnitudes across foveal, parafoveal, and peripheral vision along the horizontal meridian (55), and similar recovery times for adaptation durations ≥1,000 ms between peripheral and foveal vision (57).

Results

Experiment 1—Perifoveal Locations, Horizontal Stimulus. To investigate the adaptation effect at the vertical and horizontal meridians, we conducted a two-way ANOVA on contrast thresholds. This analysis showed a main effect of location [$F(3, 39) = 14.04$, $P < 0.001$, $\eta_p^2 = 0.52$] and a higher threshold in the adapted than nonadapted conditions [$F(1, 13) = 45.42$, $P < 0.001$, $\eta_p^2 = 0.78$], and an interaction [$F(3, 39) = 4.98$, $P = 0.005$, $\eta_p^2 = 0.28$], indicating that the adaptation effect varied across locations (Fig. 2*A*).

First, we confirmed the expected HVA and VMA in the nonadaptation condition (*SI Appendix*, Fig. S1, *Upper* panel). Contrast thresholds were lower along the horizontal than the vertical meridian [$t(13) = 5.26$, $P < 0.001$, $d = 1.41$] and lower at the lower than upper vertical meridian [$t(13) = 3.15$, $P = 0.008$, $d = 0.84$].

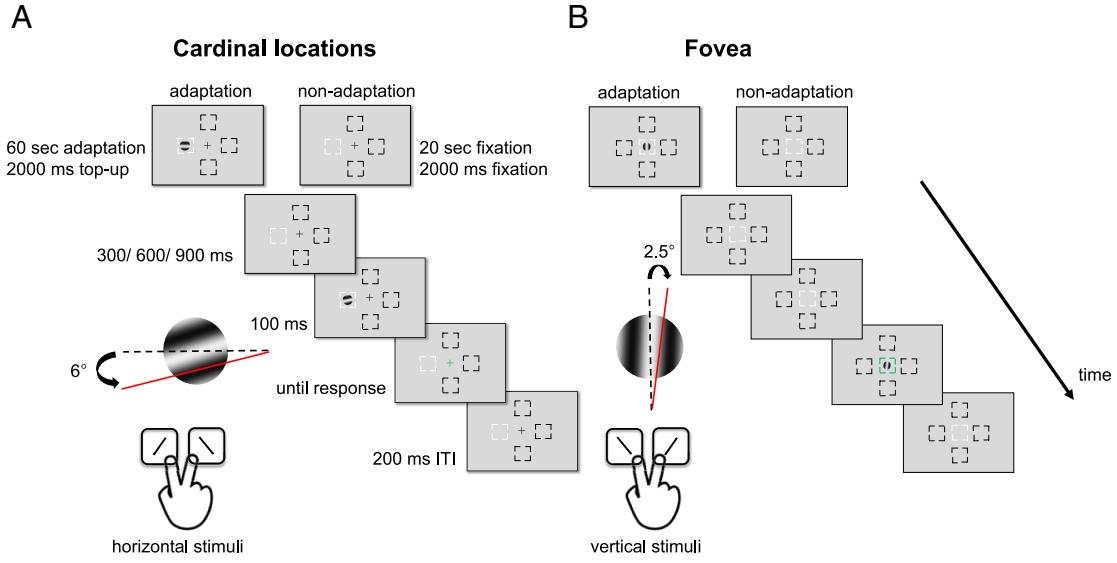

Fig. 1. (*A*) Experimental procedure: Participants performed either adaptation or nonadaptation blocks, each in separate experimental sessions. The target Gabor stimulus was always presented within the white placeholder, and target locations were blocked. The target, a horizontal (Experiment 1) or vertical (Experiment 2) Gabor stimulus, was presented either at (*A*) the perifovea (Experiments 1 and 2) or (*B*) the fovea (Experiment 3). Participants were instructed to respond whether the Gabor was tilted clockwise or counterclockwise from horizontal (Experiment 1) or vertical (Experiment 2). The target Gabor was tilted 6° from the horizontal line or 2.5° from the vertical line. For illustration purposes, the stimulus size and spatial frequency shown here are not to scale.

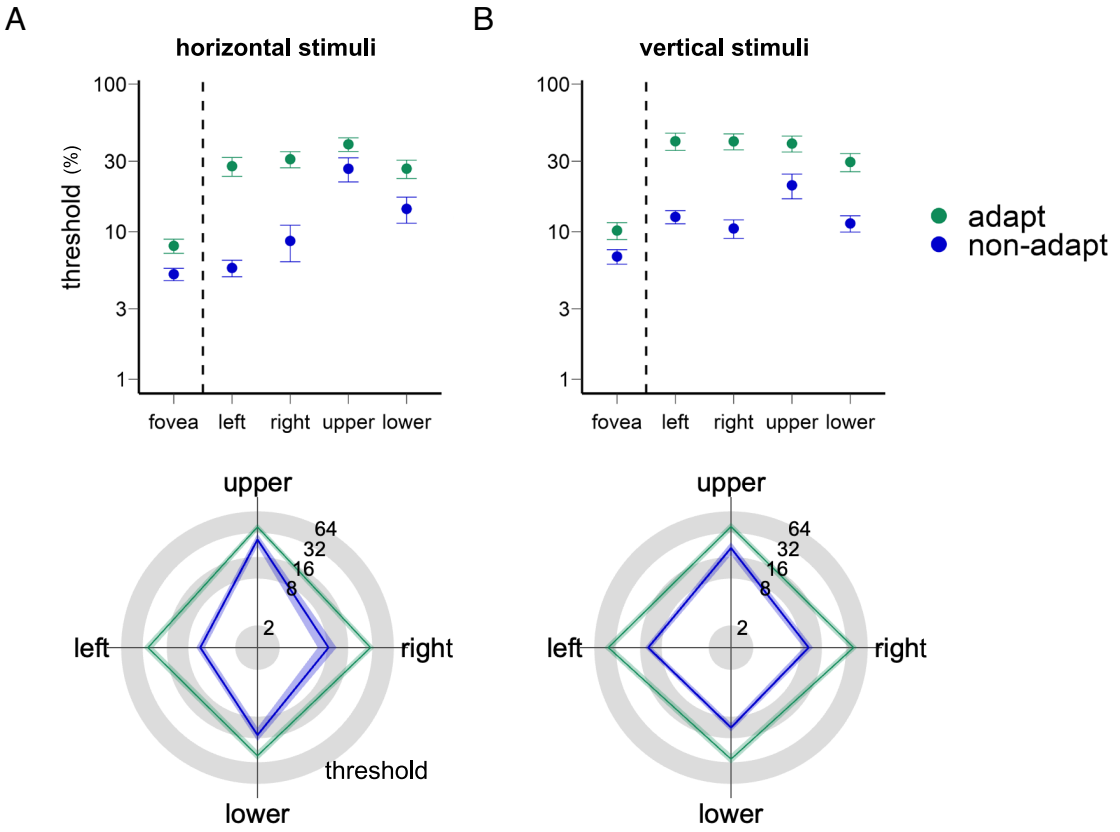

Fig. 2. The *Top* panel shows the contrast thresholds (log-scaled) for orientation discrimination at the fovea and at the *Left*, *Right*, *Upper*, and *Lower* perifoveal locations for (*A*) horizontal stimuli and (*B*) vertical stimuli. Note that for the adapted condition, contrast thresholds (%) are similar for the 4 perifoveal locations (green points). The *Bottom* panel illustrates that the adaptation effect, measured as the difference in contrast sensitivity between the adapted and nonadapted conditions, is stronger along the horizontal than the vertical meridian. The error bars represent ±1 SEM.

Next, we assessed the adaptation effect at the horizontal and vertical meridians. The adaptation effect (calculated as the difference between adapted and nonadapted thresholds, as in previous studies 112–114) was stronger at the horizontal than the vertical meridian [$t(13) = 3.77$, $P = 0.002$, $d = 1.01$] (Figs. 2*A* and 3*A*), but there was no significant difference between the upper and lower vertical meridian [$t(13) = 0.01$, $P = 0.99$].

To account for baseline differences in the nonadapted condition, we calculated a normalized adaptation effect [(adapted threshold – nonadapted threshold)/(adapted threshold + nonadapted threshold)]. This normalized adaption effect was also stronger at the horizontal than the vertical meridian [$t(13) = 7.84$, $P < 0.001$, $d = 2.1$], with no significant difference at the upper and lower vertical meridians [$t(13) = 1.3$, $P = 0.217$]. In summary, the decrease in contrast sensitivity following adaptation was more pronounced at the horizontal than the vertical meridian.

Experiment 2—Perifoveal Locations, Vertical Stimulus. When using vertical adaptor and target stimuli, the findings were consistent with those in Experiment 1. A two-way ANOVA on contrast thresholds showed main effects of location [$F(3, 39) = 4.59$, $P = 0.008$, $\eta_p^2 = 0.26$] and adaptation [$F(1, 13) = 44.15$, $P < 0.001$, $\eta_p^2 = 0.77$], as well as an interaction [$F(3, 39) = 6.63$, $P = 0.001$, $\eta_p^2 = 0.34$], indicating that the adaptation effect varied across locations (Fig. 2*B*).

In the nonadapted condition (*SI Appendix*, Fig. S1, *Lower* panel), we confirmed the expected HVA and VMA. Contrast thresholds were lower along the horizontal than the vertical meridian [$t(13) = 2.18$, $P = 0.048$, $d = 0.58$] and lower at the lower than upper vertical meridian [$t(13) = 2.57$, $P = 0.023$, $d = 0.69$].

The adaptation effect [calculated as the difference between adapted and nonadapted thresholds, as in previous studies (112–114)] was stronger at the horizontal than the vertical meridian [$t(13) = 4.04$, $P = 0.001$, $d = 1.08$] (Figs. 2*B* and 3*B*), but there was no significant difference between the upper and lower vertical meridian [$t(13) = 0.22$, $P = 0.831$]. Similarly, the normalized adaptation effect was stronger at the horizontal than the vertical meridian [$t(13) = 4.78$, $P < 0.001$, $d = 1.28$], with no significant difference between the upper and lower vertical meridians [$t(13) = 1.54$, $P = 0.147$].

Comparing Adaptation Between Stimulus Orientations. A 3-way ANOVA on contrast thresholds, with factors of location, adaptation, and stimulus orientation (horizontal: Experiment 1; vertical: Experiment 2), showed main effects of adaptation [$F(1, 13) = 54.22$, $P < 0.001$, $\eta_p^2 = 0.81$] and location [$F(3, 39) = 8.74$, $P < 0.001$, $\eta_p^2 = 0.4$], but not of stimulus orientation [$F(1, 13) = 1.25$, $P = 0.267$] or 3-way interaction [$F(3, 39) < 1$]. All two-way interactions emerged: location x orientation [$F(3, 39) = 12.33$, $P < 0.001$, $\eta_p^2 = 0.49$], adaptation × orientation [$F(1, 13) = 5.72$, $P = 0.033$, $\eta_p^2 = 0.31$], and adaptation x location [$F(3, 39) = 9.35$, $P < 0.001$, $\eta_p^2 = 0.42$].

The interaction between location and orientation (across adaptation conditions) showed a stronger HVA for horizontal than vertical stimuli [$t(13) = 4.89$, $P < 0.001$, $d = 1.31$] but no difference for the VMA [$t(13) = 1.39$, $P = 0.187$]. The interaction between adaptation and orientation (across locations) yielded a stronger adaptation effect for the vertical than horizontal stimuli [$t(13) = 2.39$, $P = 0.033$, $d = 0.64$], but this difference was not significant for the normalized adaptation effect [$t(13) = 0.78$, $P = 0.449$]. The interaction between adaptation and location (across orientations) reflected a stronger adaptation effect for horizontal than vertical

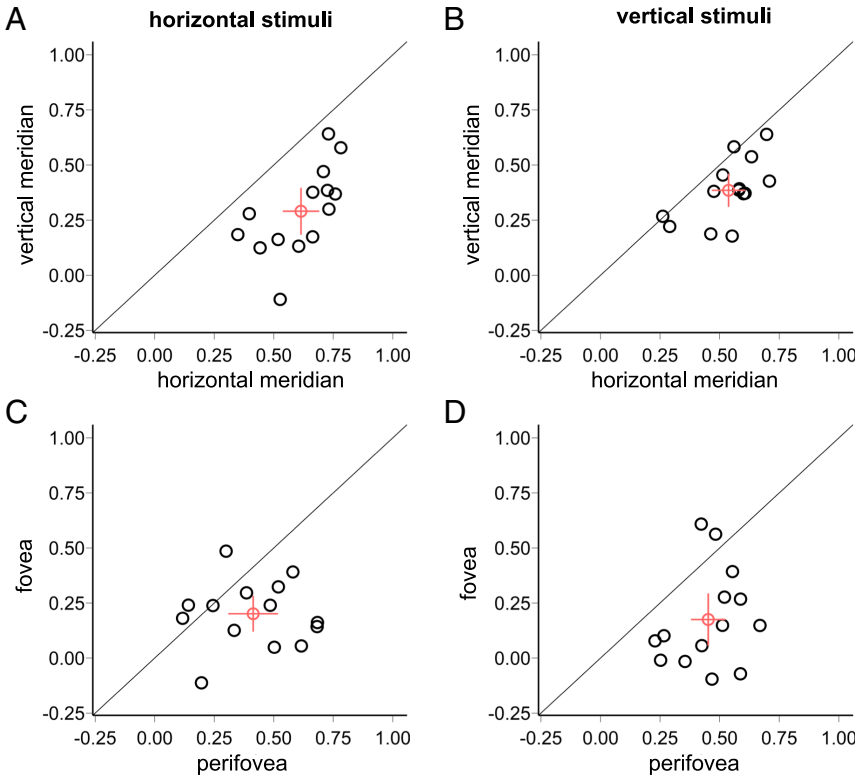

Fig. 3. *Upper* panel: Normalized adaptation effects [(adapted – nonadapted threshold)/(adapted + nonadapted threshold)] are stronger along the horizontal than the vertical meridian for both (*A*) horizontal stimuli (Experiment 1) and (*B*) vertical stimuli (Experiment 2). *Lower* panel: Adaptation effects are stronger in the perifovea than the fovea for both (*C*) horizontal and (*D*) vertical stimuli. Each black circle represents the threshold ratio for an individual participant; the red circle indicates the mean across participants. Error bars represent ±1 SEM.

locations, both without normalization [$t(13) = 5.07$, $P < 0.001$, $d = 1.36$], and with normalization [$t(13) = 7.18$, $P < 0.001$, $d = 1.92$].

The differences in HVA and VMA between horizontal and vertical stimuli under nonadapted conditions (*SI Appendix*, Fig. S1) resulted from a stronger HVA for horizontal stimuli [$t(13) = 3.83$, $P = 0.002$, $d = 1.03$, Fig. 4*A*], with no significant difference for the VMA [$t(13) = 1.04$, $P = 0.318$, Fig. 4*B*].

We observed no significant correlations between the nonadapted threshold and the adaptation effect for each participant (both Experiments 1 and 2, $ps > 0.1$) so that the extent of adaptation did not depend on the initial contrast threshold in each condition.

We found a positive correlation between normalized adaptation effects for horizontal and vertical stimuli [$r = 0.46$, $P < 0.001$, Fig. 5*A*]. To evaluate the contributions of between-observer and polar-angle variability to these correlations, we regressed out these factors as described in prior research (71). First, we accounted for between-observer variability by subtracting each observer's average adaptation effect in Experiments 1 and 2 respectively across the four polar angle locations. This correlation remained significant after removing between-observer variability [$r = 0.53$, $P < 0.001$, Fig. 5*B*]. Additionally, when we removed variability across polar angles by subtracting the average adaptation effect in Experiments 1 and 2 for each polar angle across the 14 observers, the correlation still holds [$r = 0.3$, $P = 0.026$, Fig. 5*C*]. These findings indicate that the adaptation effect was consistent with both stimulus orientations at the group and the individual levels.

In summary, the stronger HVA for horizontal stimuli aligns with a radial bias(106–108). The adaptation effect was stronger at the horizontal than the vertical meridian, regardless of the stimulus orientation.

Linking Brain and Behavior at Perifoveal Locations. To test the hypothesis that cortical surface area or pRF size is related to the adaptation effect, we assessed the relation between the normalized adaptation effect and the V1 surface area for 13 out of 14 participants (one participant preferred not to be scanned). Consistent with previous studies (70, 71, 91, 115), V1 surface area was larger along the horizontal than the vertical meridian [$t(12)=7.51$, $P < 0.001$, $d = 2.08$], and along the lower than upper vertical meridian [$t(12) = 2.37$, $P = 0.035$, $d = 0.66$, Fig. 6]. Also consistent with previous studies (70, 71), a correlation indicates that contrast threshold decreases as cortical surface area increases ($r = -0.35$, $P = 0.01$; *SI Appendix*, Fig. S2, *Left* panel), this correlation is preserved when we removed between-observer variability ($r = -0.46$, $P < 0.001$; *SI Appendix*, Fig. S2, *Middle* panel), but not when we removed polar-angle variability ($r = 0.05$,

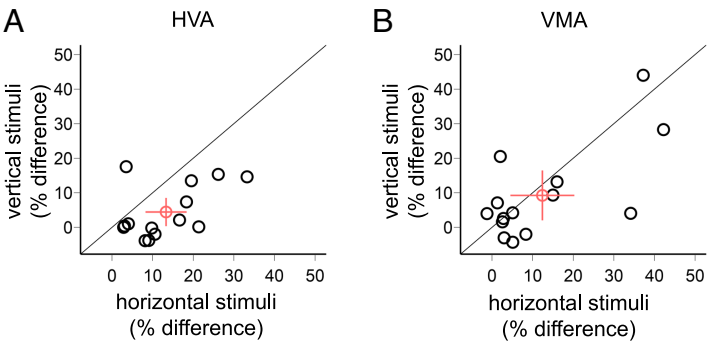

Fig. 4. Comparison of HVA (*A*) and VMA (*B*) between horizontal and vertical stimuli (% difference in contrast threshold). Each black circle represents the asymmetry for an individual participant; the red circle indicates the mean across participants. Error bars represent ±1 SEM.

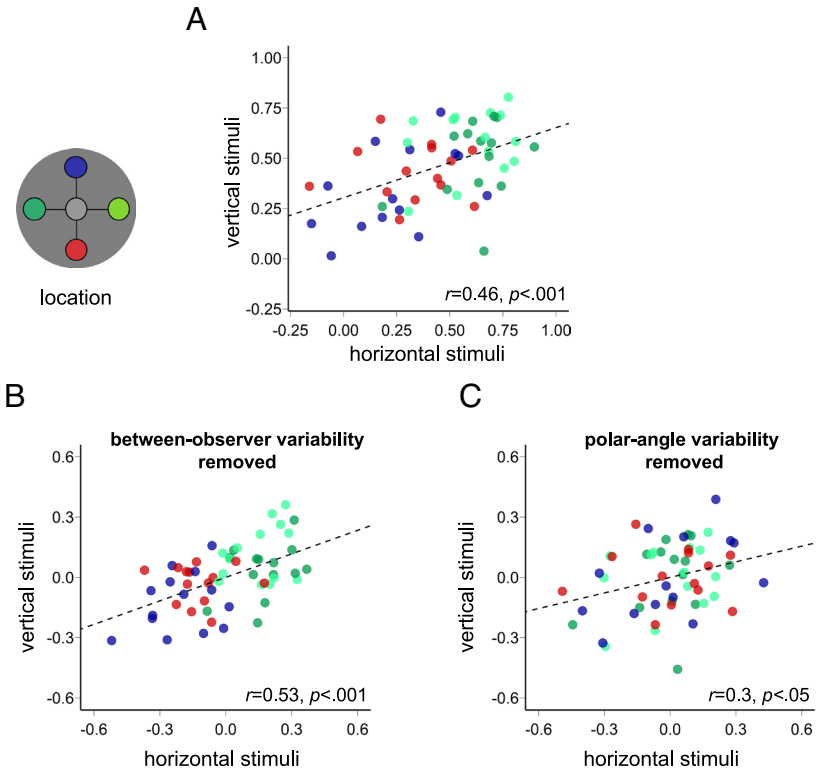

Fig. 5. (*A*) Correlation between the normalized adaptation effect [(adapted – nonadapted threshold)/(adapted + nonadapted threshold)] for the horizontal stimulus (x-axis) and the vertical stimulus (y-axis). (*B*) Correlation after removing between-subject variability. (*C*) Correlation after removing polar-angle variability. The dashed black line represents the linear fit to the data points.

P = 0.733; *SI Appendix*, Fig. S2, *Right* panel). These results highlight the importance of the polar angle.

We observed positive correlations between the normalized adaptation effect and the V1 surface area for both horizontal [r = 0.56, P < 0.001] (Fig. 7*A*) and vertical [r = 0.37, P = 0.007] (Fig. 7*B*) stimuli (*Top* panel). As this correlation relies on the variability across polar angles within the same observers, the data points are not independent. After regressing out the between-observer variability, the positive correlations persisted for both stimulus orientations (horizontal stimulus: r = 0.73, P < 0.001; vertical stimulus: r = 0.46, P < 0.001; Fig. 7, *Lower Left* panel). However, when we removed variability across polar angles, the correlations were no longer significant (horizontal stimulus: r = −0.003, P = 0.981; vertical stimulus: r = 0.07, P = 0.632; Fig. 7, *Lower Right* panel). These findings indicate that the observed correlations between the adaptation effect and V1 surface area depend on the polar angle location. Indeed, averaging the V1 surface area and adaptation effect across polar angle locations eliminated the correlations (horizontal stimulus: r = −0.19, P = 0.535; vertical stimulus: r = 0.08, P = 0.793). We observed the same patterns when correlating the non-normalized adaptation effect (computed by subtracting the thresholds) and V1 surface area (*SI Appendix*, Fig. S3).

Experiment 3—Foveal Location, Horizontal and Vertical Stimuli. The difference of cortical surface area can account for the difference of HVA but not the VMA. To further investigate the relation between V1 cortical surface area and adaptation, we examined the adaptation effect in the fovea and compared it with the one at the perifoveal locations. V1 surface area across eccentricity correlates with various perceptual measures, including perceived object size (65, 66), perceived angular size (67), and acuity (68, 69).

If the visual cortex surface area is the only determining factor of the extent of visual adaptation, the adaptation effect should be stronger at the fovea than the parafovea, and this superiority at fovea should be eliminated by adjusting the target size according to a cortical magnification factor. However, if other factors are also involved in the eccentricity difference, the adaptation effect should differ between the foveal and perifoveal locations.

A two-way ANOVA on contrast thresholds yielded main effects of adaptation [F(1, 13) = 17.69, P = 0.001, η_p^2 = 0.58] and stimulus orientation [F(1, 13) = 9.09, P = 0.01, η_p^2 = 0.41] but no interaction between them [F(1, 13) < 1]. Contrast thresholds increased after adaptation, and thresholds were lower for horizontal than vertical stimuli.

We compared the normalized adaptation effect in the fovea and the perifovea. A three-way ANOVA on adaptation x location x orientation revealed an interaction: F(1, 13) = 5.19, P = 0.04, η_p^2 = 0.29, Thus, we conducted separate two-way location × adaptation ANOVAs for horizontal and vertical stimuli.

For the horizontal stimulus, there were main effects of location [F(1, 13) = 43.93, P < 0.001, η_p^2 = 0.77] and adaptation

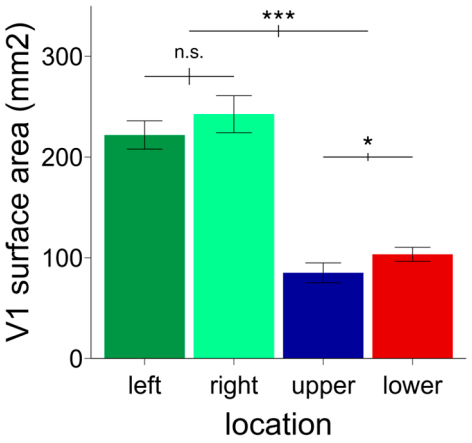

Fig. 6. V1 surface area across the four polar angle locations (extended from 4° to 12° eccentricity). Error bars represent ±1 SEM. The error bars above the bar plots indicate ±1 SEM of the difference between conditions ***P < 0.001, *P < 0.05, *n.s.* P > 0.1.

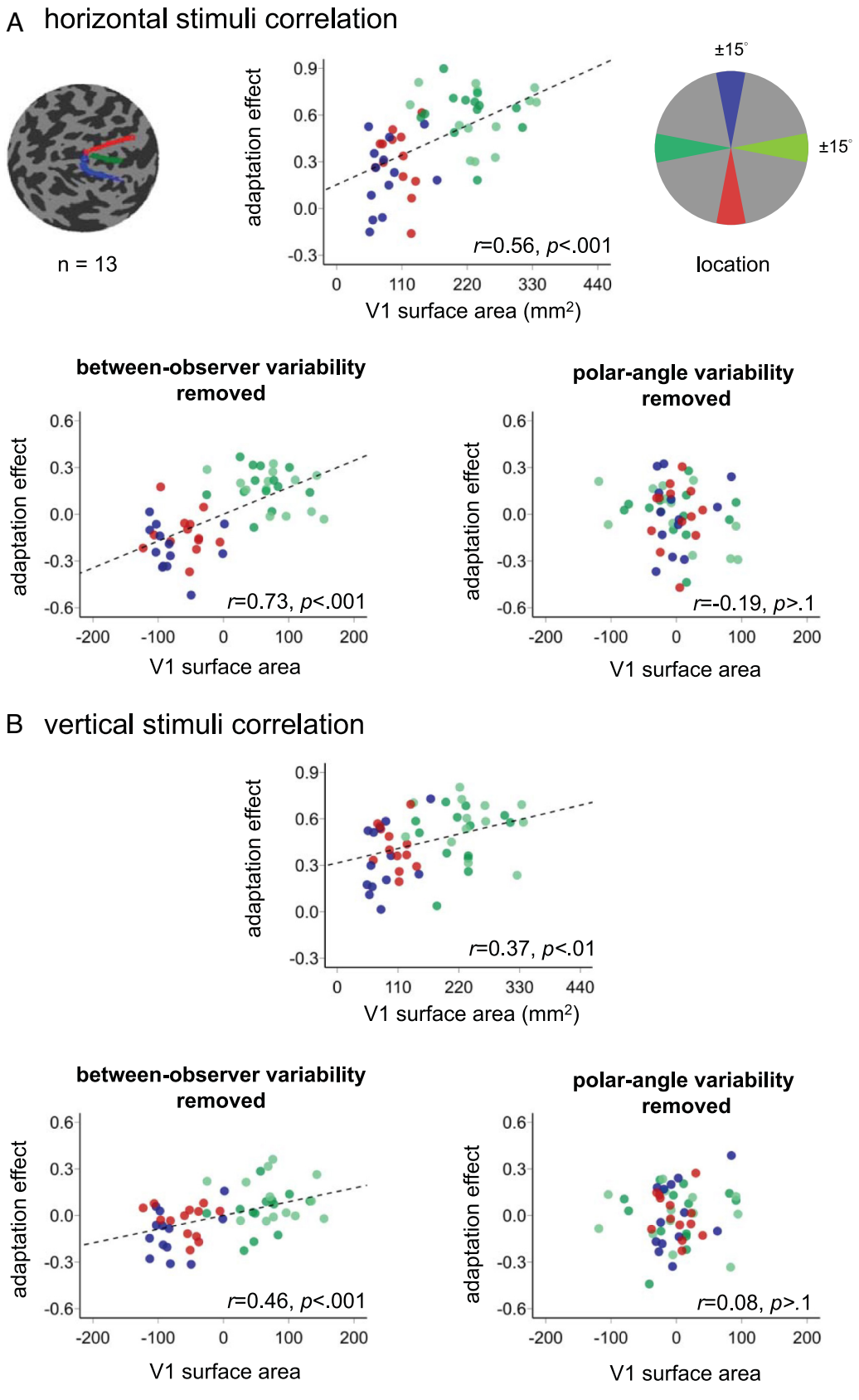

Fig. 7. Correlations between the normalized adaptation effect and V1 surface area around the polar angle for (*A*) the horizontal stimuli and (*B*) vertical stimuli. Correlations are shown overall (*Top* panels), after removing between-subject variability (*Lower Left* panels), and after removing polar-angle variability (*Lower Right* panels). The dashed black line represents the linear fit to the data points.

[$F(1, 13) = 49.25$ $P < 0.001$, $\eta_p^2 = 0.79$], as well as an interaction [$F(1, 13) = 33.72$, $P < 0.001$, $\eta_p^2 = 0.72$]. The adaptation effect [calculated as the difference between adapted and nonadapted thresholds, as in previous studies (112–114)] was stronger in the perifovea than the fovea [$t(13) = 5.58$, $P < 0.001$, $d = 1.49$]. The same result emerged for the normalized adaptation effect [$t(13) = 7.02$, $P < 0.001$, $d = 1.86$] (Figs. 2*A* and 3*C*). There was no correlation between the adaptation effect at the fovea and perifovea, either without normalization ($r = 0.25$, $P = 0.378$) or with normalization ($r = -0.08$, $P = 0.777$).

For the vertical stimulus, we observed the same patterns. There were main effects of location [$F(1, 13) = 44.81$, $P < 0.001$, $\eta_p^2 = 0.78$] and adaptation [$F(1, 13) = 41.39$, $P < 0.001$, $\eta_p^2 = 0.76$], as well as an interaction [$F(1, 13) = 34.79$, $P < 0.001$, $\eta_p^2 = 0.73$]. Again, adaptation effects were stronger in the perifovea than fovea (Figs. 2*B* and 3*D*) [$t(13) = 6.31$, $P < 0.001$, $d = 1.69$], and this was also the case for the normalized adaptation effect [$t(13) = 5.9$, $P < 0.001$, $d = 1.58$]. Additionally, there was no correlation between the adaptation effect at the fovea and perifovea, either without normalization ($r = 0.28$, $P = 0.332$) or with normalization ($r = 0.31$, $P = 0.287$).

In summary, adaptation effects were consistently stronger in the perifovea than the fovea, irrespective of stimulus orientation.

Discussion

Here, after confirming performance asymmetries in the nonadapted conditions, we uncovered stronger contrast adaptation effects at the horizontal than the vertical meridian, and in perifoveal than foveal locations, for both horizontal and vertical stimuli. These polar angle differences support our horizontal meridian dominance hypothesis: Locations with larger cortical surface areas, which contain more neurons and stronger adaptor representations (96, 97), exhibit a stronger adaptation effect (54, 98–101, 116). Critically, adaptation reduced the HVA, promoting more homogenous perception around the visual field. This differential adaptation effect was mediated by the larger cortical surface area at the horizontal than the vertical meridian.

In the nonadapted condition, we observed the typical HVA and VMA. These asymmetries likely arise from both retinal and cortical factors. For example, retinal cone density is higher at the horizontal than the vertical meridian (117, 118), midget-RGC density is higher at the lower than upper vertical meridian (118, 119), and V1 cortical surface area is larger for the horizontal than the vertical meridian, and for the lower than upper vertical meridian (Fig. 4; (63, 70–72, 91). Cortical surface area accounts for more variance in behavioral asymmetries than retinal factors (120). Additionally, factors such as sensory tuning and/or neuronal computations may also contribute to these perceptual asymmetries(3, 92, 121).

This study also revealed that the HVA, but not the VMA, was stronger for horizontal than vertical stimuli—a finding that reflects a radial bias (106–108). Horizontal stimuli favored performance along their radial (horizontal) meridian, whereas vertical stimuli favored performance along their radial (vertical) meridian, thereby respectively potentiating and diminishing the HVA.

The stronger adaptation effect for vertical stimuli (2.5° tilt) than horizontal stimuli (6° tilt)—despite matched performance, so adaptation could have the same opportunity to exert its effect in both experiments—are consistent with orientation dependency in orientation strength: adaptation decreases as the orientation difference between the target and adaptor increases (33, 39, 45, 122–126). However, normalizing the tilt angle (the difference in thresholds between the adapted and nonadapted conditions divided by their sum) eliminated orientation-related differences. Further, the adaptation effects using horizontal and vertical stimuli were positively correlated (Fig. 5*A*), regardless of between-subject (Fig. 5*B*) or polar-angle variability (Fig. 5*C*). This finding indicates that adaptation effects to two orientations had similar underpinning and were robust and reliable within individuals.

Contrast sensitivity asymmetries with this orientation discrimination task emerge at threshold (6, 10, 88) and at suprathreshold (6, 7, 88) levels. However, neither we nor anyone else has conducted adaptation experiments at suprathreshold levels around the polar angle. Thus, whether the present findings can be generalized to higher contrast levels around the polar angle remains an open question.

Prolonged exposure to an oriented stimulus causes nearby orientation to appear perceptually shifted away from the adapted orientation (e.g., 127, 128). The tilt angles used in this study were unlikely to trigger a repulsion effect because they are close to the adaptor, within a range reported to yield a slight repulsion (129), and the repulsion is typically shown when the tilt angle is around 10 to 20° (130). Had there been a repulsion effect, we would have predicted a lower threshold in the adapted than nonadapted condition; we observed the opposite. In any case, any repulsion effect would have occurred to the same extent at all tested locations. Thus, a repulsion effect could not explain the differential adaptation effect across meridians. Adaptation reduced contrast sensitivity more along the horizontal than the vertical meridian, regardless of stimulus orientation, even after normalizing the adaptation effect.

Could natural statistics play a role on this differential effect? It has been proposed that asymmetries about stimulus properties, color and orientation, are related to spatial statistics of scenes. For example, the oblique effect, better performance for horizontal and vertical than oblique lines, is related to natural statistics of the visual environment (131–135). Likewise, asymmetries in color space have been related to scene statistics (136). However, as far as we know, there is no existing evidence showing that natural statistics can explain either the horizontal–vertical meridian anisotropy (HVA) or the vertical-meridian asymmetry (VMA). Future studies should explore the contribution of scene statistics to these location asymmetries.

Why was the adaptation effect stronger along the horizontal meridian? Among the few contrast adaptation studies that specified tested locations, adaptation was either assessed throughout the entire visual field (54, 122, 126, 137) or exclusively along the horizontal meridian (55–58). To elucidate a possible mechanism underlying the stronger adaptation effect at the horizontal meridian, we consider the following points: (1) Neurostimulation studies have revealed that V1 plays a causal role in adaptation (36, 42). (2) A positive correlation exists between contrast sensitivity and V1 surface area (71). (3) V1 surface area is also positively correlated with the adaptation effect (Fig. 7, *Top* panel). This correlation persists after controlling for individual differences (Fig. 7, *Lower Left* panel), but not after accounting for polar angle variability (Fig. 7, *Lower Right* panel). (4) Neuronal density is uniform across the visual field (94, 95). Taken together, these findings suggest that the larger surface area and greater number of neurons at the horizontal than the vertical meridian contribute to the stronger adaptation effect at the horizontal meridian.

This more pronounced adaptation effect at the horizontal than the vertical meridian is also consistent with the idea that adaptation helps manage limited bioenergetic resources, as there is more expenditure for the larger cortical areas corresponding to the horizontal than the vertical meridian, and with results showing that adaptation increases with the strength of the response to the adaptor (102–105).

The surface area explanation, however, does not align well with the similar adaptation effects observed at the lower and upper vertical meridians. The surface area explanation would have predicted a stronger adaptation effect at the lower than upper vertical meridian. Thus, whereas cortical surface area can explain the decline in contrast sensitivity with increasing eccentricity, it does not fully account for polar angle differences in performance (3, 138). Together, these findings suggest that additional factors beyond surface area may contribute to the observed differential adaptation effects.

Moreover, were V1 surface area the sole factor underlying the extent of adaptation, the fovea would be expected to exhibit the strongest effect. However, in this study, even when the foveal stimulus was equated for cortical representation size (96), adaptation was weaker in the fovea than in the perifovea for both stimulus orientations. These findings are not in line with results showing that adaptation increases with the strength of the response to the adaptor (102–105). These findings are consistent with some adaptation studies (58, 59), but differ from others reporting similar adaptation effects between the fovea and periphery (40, 56). Furthermore, no correlation was observed between adaptation effects in the periphery and fovea.

Could orientation tuning play a role? The half-bandwidth of orientation selectivity is approximately 3 to 9°. In the instances in which location has been specified, these estimates are typically for foveal locations (124, 125) or for a wide eccentricity range (126). One orientation detection study showed that, for equated performance, orientation bandwidth is broader along the horizontal than the vertical meridian but similar between the upper and lower vertical meridian, demonstrating a horizontal–vertical asymmetry but not a VMA (121). Future studies could examine whether orientation tuning for adaptation varies across different meridians.

These results support the idea that foveal and peripheral vision are optimized for distinct perceptual processes (1, 2, 139). The observed differential adaptation effects are likely mediated by qualitative rather than quantitative differences in processing (58). The stronger perifoveal adaptation effect in humans is consistent with macaque studies, which show that contrast adaptation is more pronounced in the retinal and geniculate cells of the peripheral magnocellular pathway than in the more foveally located parvocellular pathway (50, 140).

Like adaptation, covert attention, the selective processing of information (2, 6, 80, 84, 86–89, 141–145), also helps manage limited resources (33–36), and these processes interact in the early visual cortex (36). However, opposite to the effect of adaptation, exogenous/involuntary (6, 7, 86, 87) or endogenous/voluntary (35, 88, 89) covert spatial(80, 146, 147) and temporal (148–150) attention enhance contrast sensitivity at the attended location. Whereas adaptation reduces the HVA, spatial (6, 7, 86–89) and temporal (149) attention enhancements are consistent around the polar angle. Thus, covert attention neither exacerbates nor alleviates the HVA or VMA.

Presaccadic attention, which enhances contrast sensitivity at the target location immediately before saccade onset, also has different effects: It enhances contrast sensitivity more along the horizontal than the vertical meridian, and least at the upper vertical meridian (151–153). Consequently, presaccadic attention can amplify polar angle asymmetries. Interestingly, individual presaccadic attention benefits negatively correlate V1 surface area at the upper vertical meridian, suggesting that presaccadic attention helps compensate for the reduced cortical surface area and neuronal count at that location (152). Similarly, the weaker adaptation effect along the vertical meridian in the present study may reflect its smaller cortical surface area and fewer neurons available for adaptation suppression.

In conclusion, this study reveals that contrast adaptation is stronger along the horizontal than the vertical meridian and in the periphery than the fovea, regardless of the adaptor and target orientation. Thus, by mitigating the HVA, adaptation contributes to reducing bioenergetic expenditure as well as inherent physiological asymmetries rendering a more uniform visual perception around the visual field. Moreover, consistent with the critical role of V1 plays in adaptation (36, 42), cortical V1 surface area mediates the differential adaptation effects observed between the horizontal and vertical meridians.

Materials and Methods

Participants. Fourteen adults (7 females, age range: 22 to 35 y old), including author HHL, participated in all three experiments. All of them had normal or corrected-to-normal vision. Sample size was based on previous studies on adaptation (36), with an effect size of $d = 1.3$, and on performance fields (151), with an effect size of $d = 1.66$ for performance in the neutral trials (without attentional manipulation). According to G*Power 3.0 (154), we would need 9 participants for adaptation and 7 participants for performance fields to reach a power = 0.9. We also estimated the required sample size for the interaction between adaptation and location, which enable us to assess performance fields, based on a presaccadic attention and performance fields study (151), as attention and adaptation both affect contrast sensitivity (155), albeit in different directions (35, 36). Bootstrapping the observers' data from that study with 10,000 iterations showed that we would need 12 participants to reach power = 0.9 for the interaction analysis. The number of participants here is similar to or higher than in previous adaptation studies (e.g., 51, 59, 144, 156, 157–160). The Institutional Review Board at New York University approved the experimental procedures, and all participants provided informed consent before they started the experiment.

Apparatus. Participants were in a dimly lit, sound-attenuated room, with their head placed on a chinrest 57 cm away from the monitor. All stimuli were generated using MATLAB (MathWorks, MA) and the Psychophysics Toolbox (161, 162) on a gamma-corrected 20-inch ViewSonic G220fb CRT monitor with a spatial resolution of 1,280 × 960 pixels and a refresh rate of 100 Hz. To ensure fixation, participants' eye movements were recorded using EYELINK 1000 (SR Research, Osgoode, Ontario, Canada) with a sample rate of 1,000 Hz.

Stimuli. In Experiments 1 and 2, the target Gabor (diameter = 4°, 5 cpd, 1.25° full-width at half maximum) was presented on the left, right, upper, and lower cardinal meridian locations (8° from the center to center). There were four placeholders (length = 0.16°, width = 0.06°) 0.5° away from Gabor's edge. The fixation cross consisted of a plus sign (length = 0.25°; width = 0.06°) at the center of the screen.

In Experiment 3, the fixation was replaced by a white placeholder, which was the same size as the other placeholders. We adjusted the target Gabor size according to the Cortical Magnification Factor (96) averaged from nasal, temporal, superior, and inferior formulas (3, 163, 164), which yielded a 1.03° diameter and presented it at the center (0° eccentricity).

Experimental Design and Procedures. Fig. 1 shows the procedure of the task. In the adaptation condition, at the beginning of each block, participants adapted to a 100%-contrast horizontal Gabor patch (5 cpd) flickering at 7.5 Hz in a counterphase manner presented at the target location for 60 s. Each trial started with 2 s top-up phase to ensure a continuous adaptation effect throughout the block. In the nonadaptation condition, participants maintained fixation at the center for 20 s (without Gabor) at the beginning of each block and for 2 s at the beginning of each trial.

After the top-up, there was a 300, 600, or 900 ms jitter before a tilted Gabor was presented for 100 ms. The fixation plus sign turned green as a response cue. Participants had to judge whether the target was tilted clockwise or counterclockwise off horizontal or vertical in Experiments 1 and 2, respectively. In Experiment 3, they responded off horizontal or vertical in different experimental sessions. The tilt angle was 6° away from the horizontal line and 2.5° away from the vertical line. They were based on pilot data to ensure a similar adaptation effect while avoiding floor or ceiling performance and were within the neurons' tuning width, the same orientation "channel" (165–167).

A feedback tone was presented when participants gave an incorrect response. The target locations were blocked. Participants were asked to respond as accurately as possible while fixating at the center of the screen throughout the trial. A trial would be aborted and repeated at the end of the block if participants' eyes position deviated ≥1.25° from the center from the onset of the adaptation top-up until the response cue onset. There were 48 trials in each block, 4 blocks

(192 trials per location for each adaptation and nonadaptation conditions) were conducted consecutively at each location.

In Experiment 1, participants completed the adaptation and nonadaptation conditions on different days, with a counterbalanced order. In Experiments 2 and 3, participants conducted the nonadapted condition followed by the adapted condition. In both Experiments 1 and 2, the order of the target locations was counterbalanced across participants. In Experiment 3, the two stimulus orientation conditions were conducted on different days (one observer the same day but an hour apart) to eliminate any carry-over effect. All observers participated in a practice session to familiarize themselves with the task procedure.

Titration Procedures. We titrated the contrast threshold of the Gabor separately for each location (central, left, right, upper, and lower) and adaptation condition (adaptation and nonadaptation) with an adaptive staircase procedure using the Palamedes toolbox (168), as in previous studies (36, 84, 151, 169). There were 4 independent staircases for each condition, varying Gabor contrast from 2% to 85% to reach ~75% accuracy for the orientation discrimination task. Each staircase started from 4 different points (85%, 2%, 43.5% the median, and a random point between 2% and 85%) and contained 48 trials. We averaged the last 8 trials to derive the contrast threshold. The few outlier staircases (3.3%), defined as the threshold 0.5 $\log_{10}$ away from the mean of other staircases in that condition (151), were excluded from data analysis.

Psychometric Function Fitting. We fitted a Weibull function for the accuracy as a function of contrast threshold. For each condition, a logistic function was fit to the data using maximum likelihood estimation using the fmincon function in MATLAB. The results derived from the psychometric function estimation positively correlated ($ps<0.01$) with the staircase results in all experiments, verifying our procedure in all conditions.

Behavioral Data Analyses. Behavioral data analyses were performed using R (170). In Experiments 1 and 2, a two-way repeated-measures ANOVA on contrast threshold was conducted on the factors of location (left, right, upper, lower) and adaptation (adapted, nonadapted) conditions to assess statistical significance. We also compared the thresholds in a three-way repeated-measures ANOVA on the factors of location (left, right, upper, lower), adaptation (adapted, nonadapted), and stimulus orientation (vertical, horizontal) across Experiments 1 and 2. In Experiment 3, we compared the contrast threshold in the fovea and periphery by pooling the performance across all locations in the periphery.

Repeated-measures ANOVA along with effect size (η^2) were computed in R (170) and used to assess statistical significance. η_p^2 was provided for all F tests, where $\eta_p^2 = 0.01$ indicates small effect, $\eta_p^2 = 0.06$ indicates a medium effect, and $\eta_p^2 = 0.14$ indicates a large effect. *Cohen's d* was also computed for each post hoc t-test, where $d = 0.2$ indicates a small effect, $d = 0.5$ indicates a medium effect, and $d = 0.8$ indicates a large effect (171).

The adaptation effect was quantified as the difference between the adapted and nonadapted threshold. We also quantified the normalized adaptation effect based on [(adapted threshold – nonadapted threshold)/(adapted threshold + nonadapted threshold)], similar to quantification of attentional effects (e.g., 100, 172, 173), which takes into account the baseline difference in the nonadapted condition.

The pRF Analysis and Correlation with the Adaptation Effect. We were able to obtain population receptive fields (pRF; 174) and anatomical data for 13 out of 14 observers from the NYU Retinotopy Database (63). One participant preferred not to be scanned. The pRF stimulus, MRI, and fMRI acquisition parameters and preprocessing, the implementation of the pRF model, and the calculation of V1 surface area were identical to those described in the previous work (3, 63, 152). In brief, we computed the amount of V1 surface area representing the left HM, right HM, upper VM, and lower VM by defining ±15° wedge-ROIs in the visual field (centered along the 4 cardinal locations) using the distance maps, as in previous studies (e.g., 71, 72). The cortical distance maps specify the distance of each vertex from the respective cardinal meridian (in mm), with the distance of the meridian itself set to 0 mm. Each ROI extended from 4° to 12° eccentricity. We did not analyze the cortical surface corresponding to the fovea because noise in the pRF estimates of retinotopic coordinates near the foveal confluence tends to be large (63, 72, 175, 176), and the fixation task covered the central 0.5° of the display during the pRF mapping measurement.

The amount of V1 surface area (in mm^2) was calculated using the average distance of a pool of vertices whose pRF polar angle coordinates lie near the edge of the 15° boundary in visual space, and we excluded vertices outside 30° away from the wedge-ROI center to preclude the noise. Two researchers (including the first author HHL) independently drew the distance maps for the dorsal and ventral part of V1 by hand using neuropythy (https://github.com/noahbenson/neuropythy; 177). The horizontal distance map was derived by the average of the dorsal and ventral maps. These steps were completed for the left and right hemispheres of V1 respectively. We then summed through the vertices that had distance within the mean distance calculated for each cardinal location. Total V1 surface area was highly consistent between independent delineations by two researchers ($r = 0.99$, $P < 0.001$). We then averaged the calculated V1 surface area between the ROIs drawn by the two researchers, as in a previous study (178), and then conducted correlation analysis to evaluate the relation between V1 surface area and the adaptation effect at the individual level.

Data, Materials, and Software Availability. Anonymized .csv data have been deposited in github (https://github.com/CarrascoLab/adaptationPF) (179).

ACKNOWLEDGMENTS. This research was supported by NIH NEI R01-EY027401 to M.C., the Ministry of Education in Taiwan to H.-H.L., and NIH NEI core grant for vision science P30EY013079 to NYU. We thank Rania Ezzo, Marc Himmbelberg, Jan Kurzawski, and David Tu for their help in fMRI data acquisition and analysis. We also thank Carrasco Lab members, especially Marc Himmelberg, Ekin Tünçok, and Shutian Xue, for their helpful comments on the manuscript.

1. H. Strasburger, I. Rentschler, M. Jüttner, Peripheral vision and pattern recognition: A review. *J. Vis.* **11**, 13 (2011).
2. K. Anton-Erxleben, M. Carrasco, Attentional enhancement of spatial resolution: Linking behavioural and neurophysiological evidence. *Nat. Rev. Neurosci.* **14**, 188–200 (2013).
3. M. Jigo, D. Tavdy, M. M. Himmelberg, M. Carrasco, Cortical magnification eliminates differences in contrast sensitivity across but not around the visual field. *eLife* **12**, e84205 (2023).
4. J. Abrams, A. Nizam, M. Carrasco, Isoeccentric locations are not equivalent: The extent of the vertical meridian asymmetry. *Vis. Res.* **52**, 70–78 (2012).
5. A. S. Baldwin, T. S. Meese, D. H. Baker, The attenuation surface for contrast sensitivity has the form of a witch's hat within the central visual field. *J. Vis.* **12**, 23 (2012).
6. E. L. Cameron, J. C. Tai, M. Carrasco, Covert attention affects the psychometric function of contrast sensitivity. *Vis. Res.* **42**, 949–967 (2002).
7. M. Carrasco, C. P. Talgar, E. L. Cameron, Characterizing visual performance fields: Effects of transient covert attention, spatial frequency, eccentricity, task and set size. *Spat. Vis.* **15**, 61 (2001).
8. J. E. Corbett, M. Carrasco, Visual performance fields: Frames of reference. *PLoS One* **6**, e24470 (2011).
9. S. Fuller, R. Z. Rodriguez, M. Carrasco, Apparent contrast differs across the vertical meridian: Visual and attentional factors. *J. Vis.* **8**, 16 (2008).
10. M. M. Himmelberg, J. Winawer, M. Carrasco, Stimulus-dependent contrast sensitivity asymmetries around the visual field. *J. Vis.* **20**, 18 (2020).
11. T. A. Nazir, Effects of lateral masking and spatial precueing on gap-resolution in central and peripheral vision. *Vis. Res.* **32**, 771–777 (1992).
12. E. Altpeter, M. Mackeben, S. Trauzettel-Klosinski, The importance of sustained attention for patients with maculopathies. *Vis. Res.* **40**, 1539–1547 (2000).
13. M. Carrasco, P. E. Williams, Y. Yeshurun, Covert attention increases spatial resolution with or without masks: Support for signal enhancement. *J. Vis.* **2**, 4 (2002).
14. C. P. Talgar, M. Carrasco, Vertical meridian asymmetry in spatial resolution: Visual and attentional factors. *Psychon. Bull. Rev.* **9**, 714–722 (2002).
15. J. A. Greenwood, M. Szinte, B. Sayim, P. Cavanagh, Variations in crowding, saccadic precision, and spatial localization reveal the shared topology of spatial vision. *Proc. Natl. Acad. Sci.* **114**, E3573–E3582 (2017).
16. T. Naito, Y. Kaneoke, N. Osaka, R. Kakigi, Asymmetry of the human visual field in magnetic response to apparent motion. *Brain Res.* **865**, 221–226 (2000).
17. L. Lakha, G. Humphreys, Lower visual field advantage for motion segmentation during high competition for selection. *Spat. Vis.* **18**, 447–460 (2005).
18. S. Fuller, M. Carrasco, Perceptual consequences of visual performance fields: The case of the line motion illusion. *J. Vis.* **9**, 13 (2009).
19. K. S. Pilz, D. Papadaki, An advantage for horizontal motion direction discrimination. *Vis. Res.* **158**, 164–172 (2019).
20. E. Tünçok, L. Kiorpes, M. Carrasco, Opposite asymmetry in visual perception of humans and macaques. *Curr. Biol.* **35**, 681–687.e4 (2024).
21. A. Barbot, S. Xue, M. Carrasco, Asymmetries in visual acuity around the visual field. *J. Vis.* **21**, 2 (2021).
22. Y. Kwak, N. M. Hanning, M. Carrasco, Presaccadic attention sharpens visual acuity. *Sci. Rep.* **13**, 2981 (2023).
23. L. Montaser-Kouhsari, M. Carrasco, Perceptual asymmetries are preserved in short-term memory tasks. *Atten. Percept. Psychophys.* **71**, 1782–1792 (2009).

24. Y. Petrov, O. Meleshkevich, Asymmetries and idiosyncratic hot spots in crowding. *Vis. Res.* **51**, 1117–1123 (2011).
25. T. S. Wallis, P. J. Bex, Image correlates of crowding in natural scenes. *J. Vis.* **12**, 6 (2012).
26. F. C. Fortenbaugh, M. A. Silver, L. C. Robertson, Individual differences in visual field shape modulate the effects of attention on the lower visual field advantage in crowding. *J. Vis.* **15**, 19 (2015).
27. J. W. Kurzawski *et al.*, The bouma law accounts for crowding in 50 observers. *J. Vis.* **23**, 6 (2023).
28. Z. Wang, Y. Murai, D. Whitney, Idiosyncratic perception: A link between acuity, perceived position and apparent size. *Proc. R. Soc. B Biol. Sci.* **287**, 20200825 (2020).
29. D. S. Schwarzkopf, Size perception biases are temporally stable and vary consistently between visual field meridians. *I-Perception* **10**, 2041669519878722 (2019).
30. A. Afraz, M. V. Pashkam, P. Cavanagh, Spatial heterogeneity in the perception of face and form attributes. *Curr. Biol.* **20**, 2112–2116 (2010).
31. M. F. Peterson, M. P. Eckstein, Individual differences in eye movements during face identification reflect observer-specific optimal points of fixation. *Psychol. Sci.* **24**, 1216–1225 (2013).
32. L.-T. Tsai, K.-M. Liao, C.-H. Hou, Y. Jang, C.-C. Chen, Visual field asymmetries in visual word form identification. *Vis. Res.* **220**, 108413 (2024).
33. A. Kohn, Visual adaptation: Physiology, mechanisms, and functional benefits. *J. Neurophysiol.* **97**, 3155–3164 (2007).
34. P. Lennie, The cost of cortical computation. *Curr. Biol.* **13**, 493–497 (2003).
35. F. Pestilli, G. Viera, M. Carrasco, How do attention and adaptation affect contrast sensitivity? *J. Vis.* **7**, 9 (2007).
36. H.-H. Lee, A. Fernández, M. Carrasco, Adaptation and exogenous attention interact in the early visual cortex: A TMS study. *iScience* **27**, 111155 (2024).
37. R. Dealy, D. Tolhurst, Is spatial adaptation an after-effect of prolonged inhibition? *J. Physiol.* **241**, 261–270 (1974).
38. D. Rose, An investigation into hemisphere differences in adaptation to contrast. *Percept. Psychophys.* **34**, 89–95 (1983).
39. A. Bradley, E. Switkes, K. De Valois, Orientation and spatial frequency selectivity of adaptation to color and luminance gratings. *Vis. Res.* **28**, 841–856 (1988).
40. S. Anstis, Adaptation to peripheral flicker. *Vis. Res.* **36**, 3479–3485 (1996).
41. D. Y. Dao, Z.-L. Lu, B. A. Dosher, Adaptation to sine-wave gratings selectively reduces the contrast gain of the adapted stimuli. *J. Vis.* **6**, 6 (2006).
42. F. Perini, L. Cattaneo, M. Carrasco, J. V. Schwarzbach, Occipital transcranial magnetic stimulation has an activity-dependent suppressive effect. *J. Neurosci.* **32**, 12361–12365 (2012).
43. M. Bao, E. Fast, J. Mesik, S. Engel, Distinct mechanisms control contrast adaptation over different timescales. *J. Vis.* **13**, 14 (2013).
44. L. Maffei, A. Fiorentini, S. Bisti, Neural correlate of perceptual adaptation to gratings. *Science* **182**, 1036–1038 (1973).
45. M. W. Greenlee, S. Magnussen, Interactions among spatial frequency and orientation channels adapted concurrently. *Vis. Res.* **28**, 1303–1310 (1988).
46. G. Sclar, P. Lennie, D. D. DePriest, Contrast adaptation in striate cortex of macaque. *Vis. Res.* **29**, 747–755 (1989).
47. M. Carandini, D. Ferster, A tonic hyperpolarization underlying contrast adaptation in cat visual cortex. *Science* **276**, 949–952 (1997).
48. M. Carandini, J. A. Movshon, D. Ferster, Pattern adaptation and cross-orientation interactions in the primary visual cortex. *Neuropharmacology* **37**, 501–511 (1998).
49. G. M. Boynton, E. M. Finney, Orientation-specific adaptation in human visual cortex. *J. Neurosci.* **23**, 8781–8787 (2003).
50. S. G. Solomon, J. W. Peirce, N. T. Dhruv, P. Lennie, Profound contrast adaptation early in the visual pathway. *Neuron* **42**, 155–162 (2004).
51. F. Fang, S. He, Viewer-centered object representation in the human visual system revealed by viewpoint aftereffects. *Neuron* **45**, 793–800 (2005).
52. T. Duong, R. D. Freeman, Spatial frequency-specific contrast adaptation originates in the primary visual cortex. *J. Neurophysiol.* **98**, 187–195 (2007).
53. M. Vergeer, J. Mesik, Y. Baek, K. Wilmerding, S. A. Engel, Orientation-selective contrast adaptation measured with SSVEP. *J. Vis.* **18**, 2 (2018).
54. J. L. Gardner *et al.*, Contrast adaptation and representation in human early visual cortex. *Neuron* **47**, 607–620 (2005).
55. A. Beaton, C. Blakemore, Orientation selectivity of the human visual system as a function of retinal eccentricity and visual hemifield. *Perception* **10**, 273–282 (1981).
56. S. Schieting, L. Spillmann, Flicker adaptation in the peripheral retina. *Vis. Res.* **27**, 277–284 (1987).
57. M. W. Greenlee, M. A. Georgeson, S. Magnussen, J. P. Harris, The time course of adaptation to spatial contrast. *Vis. Res.* **31**, 223–236 (1991).
58. Y. Gao, M. A. Webster, F. Jiang, Dynamics of contrast adaptation in central and peripheral vision. *J. Vis.* **19**, 23 (2019).
59. E. Gheorghiu, J. Bell, R. Gurnsey, Why do shape aftereffects increase with eccentricity? *J. Vis.* **11**, 18 (2011).
60. D. C. Van Essen, W. T. Newsome, J. H. Maunsell, The visual field representation in striate cortex of the macaque monkey: Asymmetries, anisotropies, and individual variability. *Vis. Res.* **24**, 429–448 (1984).
61. J. C. Horton, W. F. Hoyt, The representation of the visual field in human striate cortex: A revision of the classic Holmes map. *Arch. Ophthalmol.* **109**, 816–824 (1991).
62. S. A. Engel *et al.*, fMRI of human visual cortex. *Nature* **369**, 525–525 (1994).
63. M. M. Himmelberg *et al.*, Cross-dataset reproducibility of human retinotopic maps. *Neuroimage* **244**, 118609 (2021).
64. N. C. Benson *et al.*, Variability of the surface area of the V1, V2, and V3 maps in a large sample of human observers. *J. Neurosci.* **42**, 8629–8646 (2022).
65. D. S. Schwarzkopf, C. Song, G. Rees, The surface area of human V1 predicts the subjective experience of object size. *Nat. Neurosci.* **14**, 28–30 (2011).
66. D. S. Schwarzkopf, G. Rees, Subjective size perception depends on central visual cortical magnification in human V1. *PLoS One* **8**, e60550 (2013).
67. S. O. Murray, H. Boyaci, D. Kersten, The representation of perceived angular size in human primary visual cortex. *Nat. Neurosci.* **9**, 429–434 (2006).
68. R. O. Duncan, G. M. Boynton, Cortical magnification within human primary visual cortex correlates with acuity thresholds. *Neuron* **38**, 659–671 (2003).
69. C. Song, D. S. Schwarzkopf, R. Kanai, G. Rees, Neural population tuning links visual cortical anatomy to human visual perception. *Neuron* **85**, 641–656 (2015).
70. N. C. Benson, E. R. Kupers, A. Barbot, M. Carrasco, J. Winawer, Cortical magnification in human visual cortex parallels task performance around the visual field. *eLife* **10**, e67685 (2021).
71. M. M. Himmelberg, J. Winawer, M. Carrasco, Linking individual differences in human primary visual cortex to contrast sensitivity around the visual field. *Nat. Commun.* **13**, 3309 (2022).
72. M. M. Himmelberg *et al.*, Comparing retinotopic maps of children and adults reveals a late-stage change in how V1 samples the visual field. *Nat. Commun.* **14**, 1561 (2023).
73. J. Nachmias, Effect of exposure duration on visual contrast sensitivity with square-wave gratings. *J. Opt. Soc. Am.* **57**, 421–427 (1967).
74. Z.-L. Lu, B. A. Dosher, Spatial attention: Different mechanisms for central and peripheral temporal precues? *J. Exp. Psychol. Hum. Percept. Perform.* **26**, 1534 (2000).
75. C. Jing *et al.*, Temporal attention affects contrast response function by response gain. *Front. Hum. Neurosci.* **16**, 1020260 (2023).
76. D. Kim, S. Lokey, S. Ling, Elevated arousal levels enhance contrast perception. *J. Vis.* **17**, 14 (2017).
77. Y. Kwak, Z.-L. Lu, M. Carrasco, How the window of visibility varies around polar angle. *J. Vis.* **24**, 4 (2024).
78. Z.-L. Lu, L. A. Lesmes, B. A. Dosher, Spatial attention excludes external noise at the target location. *J. Vis.* **2**, 4 (2002).
79. H. Zheng *et al.*, Comparing spatial contrast sensitivity functions measured with digit and grating stimuli. *Transl. Vis. Sci. Technol.* **8**, 16–16 (2019).
80. F. Pestilli, S. Ling, M. Carrasco, A population-coding model of attention's influence on contrast response: Estimating neural effects from psychophysical data. *Vis. Res.* **49**, 1144–1153 (2009).
81. M. Rausch, M. Zehetleitner, Visibility is not equivalent to confidence in a low contrast orientation discrimination task. *Front. Psychol.* **7**, 591 (2016).
82. C. Roelofzen, M. Daghlian, J. A. Dijk, M. C. Jong, S. O. Dumoulin, Modeling neural contrast sensitivity functions in human visual cortex. *Imaging Neurosci.* **3**, imag_a_00469 (2025).
83. K. Herrmann, L. Montaser-Kouhsari, M. Carrasco, D. J. Heeger, When size matters: Attention affects performance by contrast or response gain. *Nat. Neurosci.* **13**, 1554–1559 (2010).
84. A. Fernández, M. Carrasco, Extinguishing exogenous attention via transcranial magnetic stimulation. *Curr. Biol.* **30**, 4078–4084.e4073 (2020).
85. H.-H. Lee, A. Fernández, M. Carrasco, Adaptation and exogenous attention interact in the early visual cortex: A TMS study. *Iscience* **27**, 111155 (2024).
86. M. Roberts, R. Cymerman, R. T. Smith, L. Kiorpes, M. Carrasco, Covert spatial attention is functionally intact in amblyopic human adults. *J. Vis.* **16**, 30 (2016).
87. M. Roberts, B. Ashinoff, F. Castellanos, M. Carrasco, Endogenous and exogenous covert attention are functionally intact in adults with ADHD. *J. Vis.* **17**, 699 (2017).
88. S. Purokayastha, M. Roberts, M. Carrasco, Voluntary attention improves performance similarly around the visual field. *Atten. Percept. Psychophys.* **83**, 2784–2794 (2021).
89. E. Tünçok, M. Carrasco, J. Winawer, Spatial attention alters visual cortical representation during target anticipation. bioXriv [Preprint] (2024). https://doi.org/10.1101/2024.03.02.583127 (Accessed 1 June 2025).
90. E. Gheorghiu, J. Bell, F. A. Kingdom, Line orientation adaptation: Local or global? *PLoS One* **8**, e73307 (2013).
91. M. F. Silva *et al.*, Radial asymmetries in population receptive field size and cortical magnification factor in early visual cortex. *Neuroimage* **167**, 41–52 (2018).
92. M. M. Himmelberg, J. Winawer, M. Carrasco, Polar angle asymmetries in visual perception and neural architecture. *Trends Neurosci.* **46**, 445–458 (2023).
93. J. Winawer, H. Horiguchi, Population receptive field size estimates in 3 human retinotopic maps. (2015). https://archive.nyu.edu/handle/2451/33887. Accessed 1 June 2025.
94. D. H. Hubel, T. N. Wiesel, Ferrier lecture-Functional architecture of macaque monkey visual cortex. *Proc. R. Soc. Lond. B Biol. Sci.* **198**, **1**–59 (1977).
95. A. Rockel, R. W. Hiorns, T. Powell, The basic uniformity in structure of the neocortex. *Brain* **103**, 221–244 (1980).
96. J. Rovamo, V. Virsu, An estimation and application of the human cortical magnification factor. *Exp. Brain Res.* **37**, 495–510 (1979).
97. A. Peters, "Number of neurons and synapses in primary visual cortex" in *Cerebral cortex: Further aspects of cortical function, including hippocampus* (Springer, 1987), pp. 267–294.
98. R. Blake, D. Tadin, K. V. Sobel, T. A. Raissian, S. C. Chong, Strength of early visual adaptation depends on visual awareness. *Proc. Natl. Acad. Sci.* **103**, 4783–4788 (2006).
99. N. A. Crowder *et al.*, Relationship between contrast adaptation and orientation tuning in V1 and V2 of cat visual cortex. *J. Neurophysiol.* **95**, 271–283 (2006).
100. T. Liu, J. Larsson, M. Carrasco, Feature-based attention modulates orientation-selective responses in human visual cortex. *Neuron* **55**, 313–323 (2007).
101. J. Larsson, A. T. Smith, fMRI repetition suppression: Neuronal adaptation or stimulus expectation? *Cereb. Cortex* **22**, 567–576 (2012).
102. N. Block, S. Siegel, Attention and perceptual adaptation (2013).
103. K. Langley, A parametric account of contrast adaptation on contrast perception. *Spat. Vis.* **16**, 77–93 (2002).
104. S. Ling, M. Carrasco, When sustained attention impairs perception. *Nat. Neurosci.* **9**, 1243–1245 (2006).
105. M. J. Spivey, M. J. Spirn, Selective visual attention modulates the direct tilt aftereffect. *Percept. Psychophys.* **62**, 1525–1533 (2000).
106. Y. Sasaki *et al.*, The radial bias: A different slant on visual orientation sensitivity in human and nonhuman primates. *Neuron* **51**, 661–670 (2006).
107. R. Ezzo, J. Winawer, M. Carrasco, B. Rokers, Asymmetries in the discrimination of motion direction around the visual field. *J. Vis.* **23**, 19 (2023).
108. J. Ryu, S.-H. Lee, Bounded contribution of human early visual cortex to the topographic anisotropy in spatial extent perception. *Commun. Biol.* **7**, 178 (2024).
109. D. Muir, R. Over, Tilt aftereffects in central and peripheral vision. *J. Exp. Psychol.* **85**, 165 (1970).
110. R. Over, J. Broerse, B. Crassini, Orientation illusion and masking in central and peripheral vision. *J. Exp. Psychol.* **96**, 25 (1972).
111. J. Harris, J. Calvert, Contrast, spatial frequency and test duration effects on the tilt aftereffect: Implications for underlying mechanisms. *Vis. Res.* **29**, 129–135 (1989).
112. M. Georgeson, Apparent spatial frequency and contrast of gratings: Separate effects of contrast and duration. *Vis. Res.* **25**, 1721–1727 (1985).
113. M. W. Greenlee, F. Heitger, The functional role of contrast adaptation. *Vis. Res.* **28**, 791–797 (1988).

114. A. M. McKendrick, G. P. Sampson, M. J. Walland, D. R. Badcock, Impairments of contrast discrimination and contrast adaptation in glaucoma. *Invest. Ophthalmol. Vis. Sci.* **51**, 920–927 (2010).
115. C. O'Connell *et al.*, Structural and functional correlates of visual field asymmetry in the human brain by diffusion kurtosis MRI and functional MRI. *Neuroreport* **27**, 1225–1231 (2016).
116. E. Tring, M. Dipoppa, D. L. Ringach, On the contrast response function of adapted neural populations. *J. Neurophysiol.* **131**, 446–453 (2024).
117. C. A. Curcio, K. R. Sloan Jr., O. Packer, A. E. Hendrickson, R. E. Kalina, Distribution of cones in human and monkey retina: Individual variability and radial asymmetry. *Science* **236**, 579–582 (1987).
118. C. A. Curcio, K. R. Sloan, R. E. Kalina, A. E. Hendrickson, Human photoreceptor topography. *J. Comp. Neurol.* **292**, 497–523 (1990).
119. H. Song, T. Y. P. Chui, Z. Zhong, A. E. Elsner, S. A. Burns, Variation of cone photoreceptor packing density with retinal eccentricity and age. *Invest. Ophthalmol. Vis. Sci.* **52**, 7376–7384 (2011).
120. E. R. Kupers, N. C. Benson, M. Carrasco, J. Winawer, Asymmetries around the visual field: From retina to cortex to behavior. *PLoS Comput. Biol.* **18**, e1009771 (2022).
121. S. Xue, M. Carrasco, Featural representation underlies performance differences around the visual field. *J. Vis.* **23**, 4771 (2023).
122. F. Fang, S. O. Murray, D. Kersten, S. He, Orientation-tuned fMRI adaptation in human visual cortex. *J. Neurophysiol.* **94**, 4188–4195 (2005).
123. C. Blakemore, J. Nachmias, The orientation specificity of two visual after-effects. *J. Physiol.* **213**, 157–174 (1971).
124. R. J. Snowden, Measurement of visual channels by contrast adaptation. *Proc. R. Soc. Lond. B Biol. Sci.* **246**, 53–59 (1991).
125. G. C. Phillips, H. R. Wilson, Orientation bandwidths of spatial mechanisms measured by masking. *J. Opt. Soc. Am. A, Opt. Image Sci. Vis.* **1**, 226–232 (1984).
126. J. Larsson, S. J. Harrison, Spatial specificity and inheritance of adaptation in human visual cortex. *J. Neurophysiol.* **114**, 1211–1226 (2015).
127. J. J. Gibson, M. Radner, Adaptation, after-effect and contrast in the perception of tilted lines. I. Quantitative studies. *J. Exp. Psychol.* **20**, 453 (1937).
128. T. Tzvetanov, A. Wirmer, K. Folta, Orientation repulsion and attraction in alignment perception. *Vis. Res.* **47**, 1693–1704 (2007).
129. B. O'Toole, P. Wenderoth, The tilt illusion: Repulsion and attraction effects in the oblique meridian. *Vis. Res.* **17**, 367–374 (1977).
130. C. W. Clifford, The tilt illusion: Phenomenology and functional implications. *Vis. Res.* **104**, 3–11 (2014).
131. N. D. Bruce, J. K. Tsotsos, A statistical basis for visual field anisotropies. *Neurocomputing* **69**, 1301–1304 (2006).
132. S. C. Dakin, I. Mareschal, P. J. Bex, Local and global limitations on direction integration assessed using equivalent noise analysis. *Vis. Res.* **45**, 3027–3049 (2005).
133. S. Nasr, R. B. Tootell, A cardinal orientation bias in scene-selective visual cortex. *J. Neurosci.* **32**, 14921–14926 (2012).
134. A. R. Girshick, M. S. Landy, E. P. Simoncelli, Cardinal rules: Visual orientation perception reflects knowledge of environmental statistics. *Nat. Neurosci.* **14**, 926–932 (2011).
135. A. M. Hussain Ismail, J. A. Solomon, M. Hansard, I. Mareschal, *A tilt after-effect for images of buildings: Evidence of selectivity for the orientation of everyday scenes* (Royal Society Open Science, 2016), **vol. 3**, p. 160551.
136. M. A. Webster, Y. Mizokami, S. M. Webster, Seasonal variations in the color statistics of natural images. *Network Comput. Neural Syst.* **18**, 213–233 (2007).
137. L. N. Vinke, I. M. Bloem, S. Ling, Saturating nonlinearities of contrast response in human visual cortex. *J. Neurosci.* **42**, 1292–1302 (2022).
138. S. Xue, A. Fernández, M. Carrasco, Featural representation and internal noise underlie the eccentricity effect in contrast sensitivity *J. Neurosci.* **44**, e0743232023 (2024)
139. R. Rosenholtz, Capabilities and limitations of peripheral vision. *Annu. Rev. Vis. Sci.* **2**, 437–457 (2016).
140. A. J. Camp, C. Tailby, S. G. Solomon, Adaptable mechanisms that regulate the contrast response of neurons in the primate lateral geniculate nucleus. *J. Neurosci.* **29**, 5009–5021 (2009).
141. T. van Mourik, P. J. Koopmans, L. J. Bains, D. G. Norris, J. F. Jehee, Investigation of layer-specific BOLD signal in the human visual cortex during visual attention. *Aperture Neuro* **3**, 1–18 (2023).
142. S. Crespi *et al.*, Spatiotopic coding of BOLD signal in human visual cortex depends on spatial attention *PLoS One* **6**, e21661 (2011).
143. M. C. Morrone, V. Denti, D. Spinelli, Different attentional resources modulate the gain mechanisms for color and luminance contrast. *Vis. Res.* **44**, 1389–1401 (2004).
144. A. Barbot, M. Carrasco, Attention modifies spatial resolution according to task demands. *Psychol. Sci.* **28**, 285–296 (2017).
145. M. Roberts, B. K. Ashinoff, F. X. Castellanos, M. Carrasco, When attention is intact in adults with ADHD. *Psychon. Bull. Rev.* **25**, 1423–1434 (2018).
146. S. Ling, M. Carrasco, Sustained and transient covert attention enhance the signal via different contrast response functions. *Vis. Res.* **46**, 1210–1220 (2006).
147. F. Pestilli, M. Carrasco, Attention enhances contrast sensitivity at cued and impairs it at uncued locations. *Vis. Res.* **45**, 1867–1875 (2005).
148. R. N. Denison, D. J. Heeger, M. Carrasco, Attention flexibly trades off across points in time. *Psychon. Bull. Rev.* **24**, 1142–1151 (2017).
149. A. Fernández, R. N. Denison, M. Carrasco, Temporal attention improves perception similarly at foveal and parafoveal locations. *J. Vis.* **19**, 12 (2019).
150. R. N. Denison, Visual temporal attention from perception to computation. *Nat. Rev. Psychol.* **3**, 261–274 (2024).
151. N. M. Hanning, M. M. Himmelberg, M. Carrasco, Presaccadic attention enhances contrast sensitivity, but not at the upper vertical meridian. *Iscience* **25**, 103851 (2022).
152. N. M. Hanning, M. M. Himmelberg, M. Carrasco, Presaccadic attention depends on eye movement direction and is related to V1 cortical magnification. *J. Neurosci.* **44**, e1023232023 (2024).
153. Y. Kwak, Y. Zhao, Z.-L. Lu, N. M. Hanning, M. Carrasco, Presaccadic attention enhances and reshapes the contrast sensitivity function differentially around the visual field. *ENeuro* **11**, ENEURO.0243-24.2024 (2024).
154. F. Faul, E. Erdfelder, A.-G. Lang, A. Buchner, G* Power 3: A flexible statistical power analysis program for the social, behavioral, and biomedical sciences. *Behav. Res. Methods* **39**, 175–191 (2007).
155. M. Carrasco, Visual attention: The past 25 years. *Vis. Res.* **51**, 1484–1525 (2011).
156. S.-L. Yeh, I. Chen, K. K. De Valois, R. L. De Valois, Figural aftereffects and spatial attention. *J. Exp. Psychol. Hum. Percept. Perform.* **22**, 446 (1996).
157. D. Melcher, Spatiotopic transfer of visual-form adaptation across saccadic eye movements. *Curr. Biol.* **15**, 1745–1748 (2005).
158. A. Ezzati, A. Golzar, A. S. Afraz, Topography of the motion aftereffect with and without eye movements. *J. Vis.* **8**, 23 (2008).
159. K. Anton-Erxleben, K. Herrmann, M. Carrasco, Independent effects of adaptation and attention on perceived speed. *Psychol. Sci.* **24**, 150–159 (2013).
160. S. L. Fairhall, J. Schwarzbach, A. Lingnau, M. G. Van Koningsbruggen, D. Melcher, Spatiotopic updating across saccades revealed by spatially-specific fMRI adaptation. *Neuroimage* **147**, 339–345 (2017).
161. D. H. Brainard, The psychophysics toolbox. *Spat. Vis.* **10**, 433–436 (1997).
162. D. G. Pelli, The videotoolbox software for visual psychophysics: Transforming numbers into movies. *Spat. Vis.* **10**, 437–442 (1997).
163. M. Carrasco, T. L. McLean, S. M. Katz, K. S. Frieder, Feature asymmetries in visual search: Effects of display duration, target eccentricity, orientation and spatial frequency. *Vis. Res.* **38**, 347–374 (1998).
164. S. J. Prince, B. J. Rogers, Sensitivity to disparity corrugations in peripheral vision. *Vis. Res.* **38**, 2533–2537 (1998).
165. C. Blakemore, F. W. Campbell, On the existence of neurones in the human visual system selectively sensitive to the orientation and size of retinal images. *J. Physiol.* **203**, 237–260 (1969).
166. V. Dragoi, J. Sharma, M. Sur, Adaptation-induced plasticity of orientation tuning in adult visual cortex. *Neuron* **28**, 287–298 (2000).
167. K. Herrmann, D. J. Heeger, M. Carrasco, Feature-based attention enhances performance by increasing response gain. *Vis. Res.* **74**, 10–20 (2012).
168. N. Prins, F. A. Kingdom, Applying the model-comparison approach to test specific research hypotheses in psychophysical research using the Palamedes toolbox. *Front. Psychol.* **9**, 1250 (2018).
169. M. Jigo, M. Carrasco, Attention alters spatial resolution by modulating second-order processing. *J. Vis.* **18**, 2 (2018).
170. R. C. Team, R language definition. *Vienna, Austria: R Foundation for Statistical Computing* **3**, 116 (2000).
171. J. Cohen, *Statistical Power Analysis for the Behavioral Sciences* (Routledge, 2013).
172. E. A. Buffalo, P. Fries, R. Landman, H. Liang, R. Desimone, A backward progression of attentional effects in the ventral stream. *Proc. Natl. Acad. Sci.* **107**, 361–365 (2010).
173. A. M. Ni, J. H. Maunsell, Spatially tuned normalization explains attention modulation variance within neurons. *J. Neurophysiol.* **118**, 1903–1913 (2017).
174. S. O. Dumoulin, B. A. Wandell, Population receptive field estimates in human visual cortex. *Neuroimage* **39**, 647–660 (2008).
175. R. F. Dougherty *et al.*, Visual field representations and locations of visual areas V1/2/3 in human visual cortex. *J. Vis.* **3**, 1 (2003).
176. M. M. Schira, C. W. Tyler, M. Breakspear, B. Spehar, The foveal confluence in human visual cortex. *J. Neurosci.* **29**, 9050–9058 (2009).
177. N. C. Benson, J. Winawer, Bayesian analysis of retinotopic maps. *eLife* **7**, e40224 (2018).
178. J. W. Kurzawski *et al.*, Human V4 size predicts crowding distance. *Nat. Commun.* **16**, 3876 (2025).
179. H. H. Lee, M. Carrasco, Visual adaptation stronger at the horizontal than the vertical meridian: Linking performance with V1 cortical surface area. Github. https://github.com/CarrascoLab/adaptationPF. Deposited 9 January 2025.